

Control Mechanism of an Organic Self-Regulating Microfluidic System

Sanghoon Lee, David T. Eddington, Youngmin Kim, Woosung Kim, and David J. Beebe, *Member, IEEE*

Abstract—The control mechanism and fluid dynamic properties of a previously developed organic pH regulation system are analyzed. The system regulates an output fluid stream to a pH of 6.7 with varying input flow rates. A pH sensitive hydrogel post acts as the feedback pH sensor and flow regulator. The control mechanism of the system is studied through numerical modeling of the regulator and the model is validated through experimentation. Analysis of the fluid dynamics at a T-channel junction, in which two buffer streams merge into one, is performed by solving the Navier-Stokes equation with commercial software. Various areas of a star-shaped orifice are occluded by a flexible membrane to throttle the rate that compensating buffer is fed back into the system. The relationship between orifice open area and volume of compensating buffer through the orifice was analyzed numerically. The axial and lateral visualization of the hydrogel post was obtained via optical microscopy. The model of the regulation system successfully predicts experimental results. [957]

Index Terms—Analytical modeling, CFD, hydrogel, organic self-regulating.

I. INTRODUCTION

ORGANIC mechanisms control the human body at all scales, from the whole body down to the single cell. The demonstration of self regulating and biocompatible systems that mimic natural regulation is an area of active research in microfluidics. Microfluidic systems have advantages over macro systems due to reduced diffusion times associated with their smaller size. The dimensions of silicon based microelectromechanical systems (MEMS) are on the order of a single cell. Examples of MEMS technology include microsensors [1]–[3], fluid control devices [4], [5] cell separation tools [6], flow injection reaction analysis [7], cell patterning devices [8] and cell manipulators [9]. However, silicon-based devices increase system complexity and manufacturing difficulty when an electrically driven feedback control system is employed. Electrical feedback systems require micro sensors, amplifier circuits, micro-actuators, microprocessors and peripheral circuits, in contrast to the human body that is controlled through efficient

biochemical mechanisms. So, interest in organic microsystems without electrical components is growing in the fields of biotechnology and clinical medicine. Recently, polymer based microsystems utilizing soft actuators and plumbing have been employed to replace silicon based devices due to lower cost and shorter fabrication times as compared with traditional MEMS. Polymer based microsystems have diverse applications in the field of biotechnology [10], [11]. Specifically, stimulus responsive hydrogels have many applications including , valves [12], drug delivery actuators [13], self-regulating devices [14] and artificial muscles [15]. Responsive hydrogels are polymers whose swelling behavior is sensitive to changes in environmental conditions which can be classified according to the stimuli they respond to as: temperature [16], pH [17], electric [18], light [19], glucose [20], antigen [21] and magnetic field [22] sensitive, with some responding to multiple stimuli. In pH sensitive hydrogels the polymer network changes from neutral to charged due to protonation of amine groups or deprotonation of acid groups. After the protonation or deprotonation, the hydrogel undergoes a volume transition from the collapsed state to the expanded state due to osmotic pressure exerted by mobile counter-ions neutralizing the fixed network charges within the hydrogel network [23]. One important application for pH responsive hydrogels is to control the temporal release of pharmaceuticals.

Recently, pH control and regulation systems that do not require any electrical control components have been demonstrated [12], [14]. In the regulation system, a stimulus responsive polymeric material replaces the major components (micro sensor, micro actuator, microprocessor and peripheral circuits) required for a conventional microfluidic pH regulation system. To incorporate the responsive hydrogel post (diameter: 350 μm) into the three-dimensional (3-D) microfluidic network, *in-situ* photopolymerization is utilized [25]. The microfluidic device can be constructed within one day and feedback control is achieved while maintaining system elegance (diverse functionality and ease of construction) through the use of hybrid system designs combining a 3-D micromolded channel network with *in situ* construction of stimuli responsive components. The pH self-regulating system demonstrated stable control of the pH of a microfluidic stream under a range of input flow conditions [14].

The objective of the current study is to analyze the control mechanisms of the pH regulation system by comparing simulations and experiments. To make the numerical simulation model, a block diagram of the system is established with the pH responsive hydrogel post as the feedback element. The numerical model of each block in the simulation is obtained by theoretical and experimental methods. The property of fluid flow

Manuscript received November 5, 2002; revised July 25, 2003. Subject Editor A. J. Ricco.

S. Lee is with the Department of Biomedical engineering, Dankook University, Cheonan, 330-714, Korea and also with the Department of Biomedical Engineering, University of Wisconsin-Madison, Madison, WI 53706 USA (e-mail: dbiomed@dankook.ac.kr).

D. T. Eddington and D. J. Beebe are with the Department of Biomedical Engineering, University of Wisconsin-Madison, Madison, WI 53706 USA (e-mail: dbeebe@engr.wisc.edu).

Y. Kim and W. Kim are with the Department of Mechanical Engineering, Hanyang University, Ansan 425-791, Korea (e-mail: wskim@hanyang.ac.kr).

Digital Object Identifier 10.1109/JMEMS.2003.820292

in the microchannel is analyzed with computational fluid dynamics (CFD) software based on Navier–Stokes equations. The performance of the pH regulation system model was evaluated through experiments.

II. SYSTEM OPERATION

The pH regulation system consists of a hydrogel post, PDMS membrane, star-shaped orifice and mixing T-channel as shown in Fig. 1. The system is fabricated as described previously [14]. Two inlet channels enter the device with one channel supplying acidic (pH 2) solution and the other channel supplying a compensating basic (pH 12) solution. The two inlet flows are driven by a water column. The pressure at the input channel is varied from 10 cmH₂O to 50 cmH₂O, while pressure at the compensating channel is fixed at 50 cmH₂O. The dimensions of the input channel and output channel are 200 × 170 μm and the compensating channel is 200 × 100 μm. Due to the size of the channels and pressures applied, the flow remains laminar as it travels past the hydrogel. The input and compensating streams are stacked vertically causing the top of the gel to be constantly exposed to acidic solution and the bottom exposed to basic solution. However, the pH is measured at the outlet of the device and assumed to be totally mixed due to the dimensions of the outlet. A pressure increase at the input causes the elevation of input flow and the pH at the output channel becomes more acidic. As the hydrogel shrinks in the acidic solution, the membrane seals off a smaller area of the star orifice, allowing more compensating buffer solution to pass through the orifice as shown in Fig. 2. The increased compensating solution increases the pH of the output channel, causing the hydrogel post to swell and decrease the amount of compensating buffer solution allowed to pass through the orifice. The time response of the system was found to be about five minutes.

III. MODELING OF THE PH REGULATION SYSTEM

Key components of the pH regulation system include a T-channel, hydrogel post, membrane, and star-shaped orifice as shown in Fig. 1. Since the pH at the output channel is determined by the flow ratio of the two inlet channels, a pH converter (relating flow ratio to output pH) is incorporated in the numerical model. Fig. 3 shows the block diagram with the T-channel and pH converter included in the feed-forward loop and the hydrogel post and star-shaped orifice in the feedback loop. The T-channel mixes the solutions from the input and compensating channels at a rate determined from the dimensions and applied pressure of each channel. The modeling of the pH converter and the shrinking and swelling properties of the hydrogel post are experimentally investigated. The star-shaped orifice, membrane and hydrogel post regulates the feedback flow. Assuming the membrane is thin and sufficiently flexible, the influence of the membrane on the hydrogel post can be ignored. The saturator models the limit on compensating solution flow due to physical effects (channel size, driving pressure). The numerical model was implemented in Simulink (MatLab 6.0).

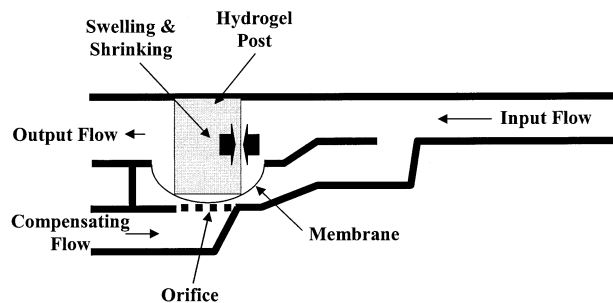


Fig. 1. Schematic diagram of the pH self-regulating system. Cross-sectional area of input and output channel : 200 × 170 μm, and compensating channel: 200 × 100 μm. Distance from the T-intersection to the center of hydrogel post: 4.4 mm. Diameter of hydrogel post: 350 μm.

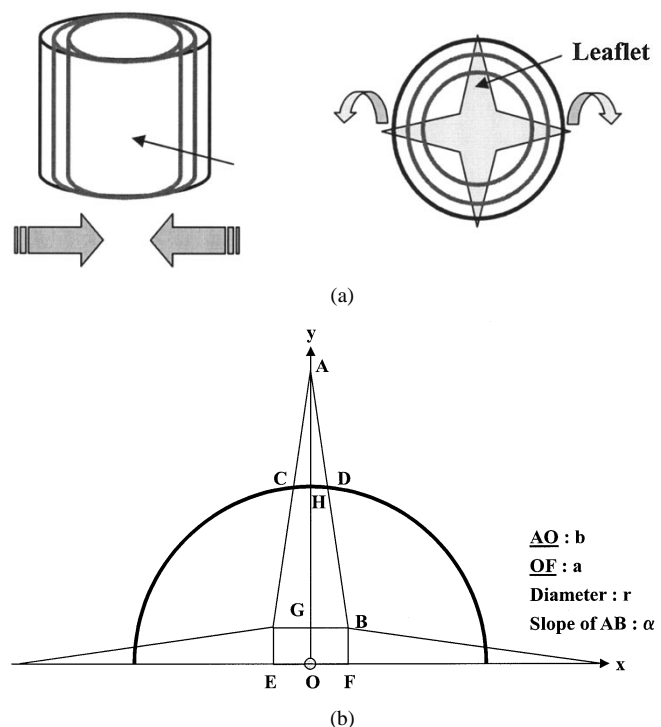


Fig. 2. (a) Schematic explaining the relationship between hydrogel size and open orifice area. (b) Geometrical model of the hydrogel post and orifice.

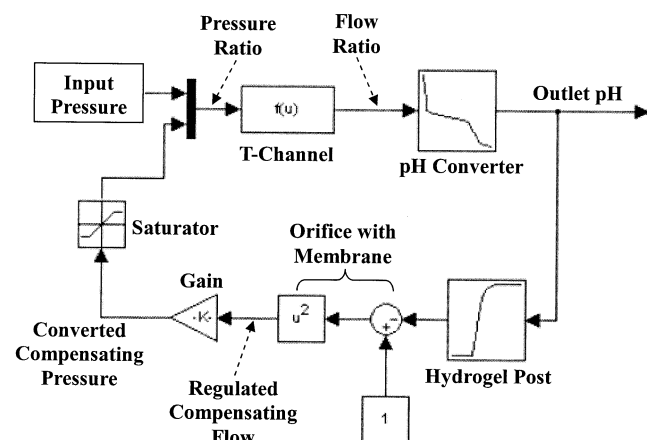


Fig. 3. Block diagram of the self pH regulating system implemented on Simulink.

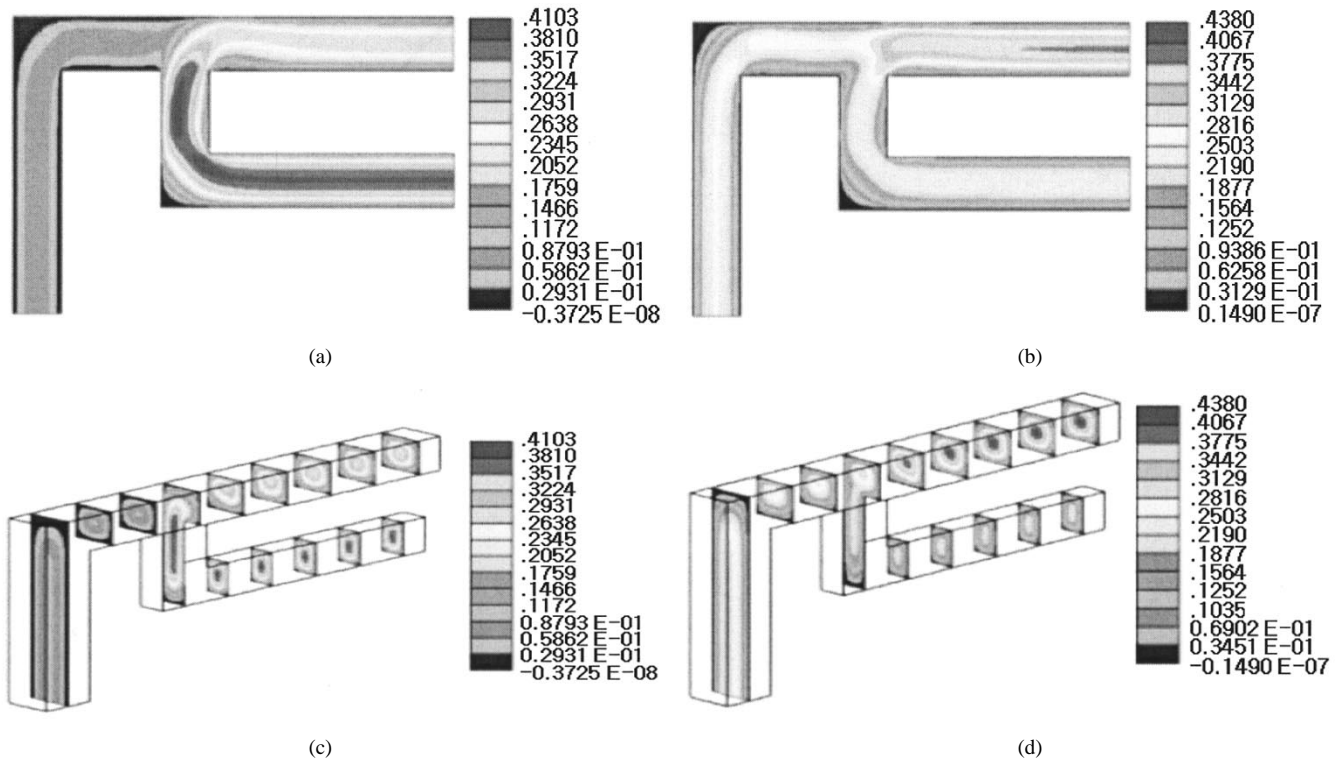


Fig. 4. Plot of velocity magnitude contour with (a) Input channel: 30 cmH₂O, compensating channel: 50 cmH₂O and (b) Input channel: 50 cmH₂O, compensating channel: 50 cmH₂O and Plot of multi-section slice contour (c) Input channel: 30 cmH₂O, compensating channel: 50 cmH₂O and (d) Input channel: 50 cmH₂O, compensating channel: 50 cmH₂O.

A. Fluid Dynamics in T-Channel

The size of microsystems causes different fluid flow properties than flow in macrosystems. In conventional fluid dynamic theory, Navier–Stokes equations with no slip conditions are used to predict flow properties with close correlation to experiments. A number of flow characteristics normally ignored in conventional macro flow, must be considered at the microscale to achieve accurate simulations.

A fundamental understanding of the flow characteristics of the regulation system, such as velocity and pressure distribution, is critical to the performance optimization. For the numerical simulation of a T-channel, a geometric model of the pH regulation system was established, and the simulation was carried out using a commercially available modeling package (STAR CD, CD-Adapco). Body-fitted structured grids are used and the total number of cells is approximately 12 000 in all cases. The Semi-Implicit Pressure-Linked Equation (SIMPLE) method is implemented for pressure-velocity coupling.

In the model, the pressure at the inlet was changed from 30, 40, 50, and 60 cmH₂O while the compensating pressure was fixed at 50 cmH₂O. Fig. 4 is representative modeling results showing velocity contours for two distinct cases. The first case [see Fig. 4(a)] has an input and compensating pressure of 30 cmH₂O and 50 cmH₂O respectively, while the second case [see Fig. 4(b)] has the input and compensating pressures at 50 cmH₂O and 50 cmH₂O respectively. As the pressure of the input channel increases, the flow fraction from the inlet channel becomes higher and the pH at the output channel becomes more acidic. In contrast, a decrease in input pressure makes the output solution more basic. The velocity multi-section

contour is shown in Fig. 4(c) and (d) and the effect of pressure in the inlet channel can be clearly seen at the mixing position of the T-channel. The average flow velocity of both channels is calculated using the following equation:

$$\bar{V} = \frac{\int_A \rho \vec{V} \cdot \hat{n} dA}{\rho A} \quad (1)$$

\bar{V} : mean velocity, \vec{V} : velocity, ρ : density, \hat{n} : normal vector to the surface, A : cross-sectional area of channel.

Fig. 5 shows the ratio of fractional flows at the output channel when the applied pressure at the input channel changes from 30 cmH₂O to 60 cmH₂O and the compensating channel driving pressure is fixed at 50 cmH₂O.

B. Modeling of pH Converter

The pH at the output is determined by the ratio of two solutions with different pH values. Phosphate buffer with ionic strength adjusted to 0.2 M through the addition of NaCl was used in the experiment at pH 2 (inlet) and pH 12 (compensating). To obtain a relationship between flow ratio and pH, the two solutions are mixed with different volume ratios and a microcombination pH electrode (PHR-146, LAZAR) measures the pH of the mixed solution and the relationship between the flow ratio and pH is obtained. Piecewise linearization was used to obtain the transfer function relating flow ratio to pH at the output channel and the equations are as follows:

$$y = -14.1x + 12 \quad \left(x \leq \frac{1}{3} \right)$$

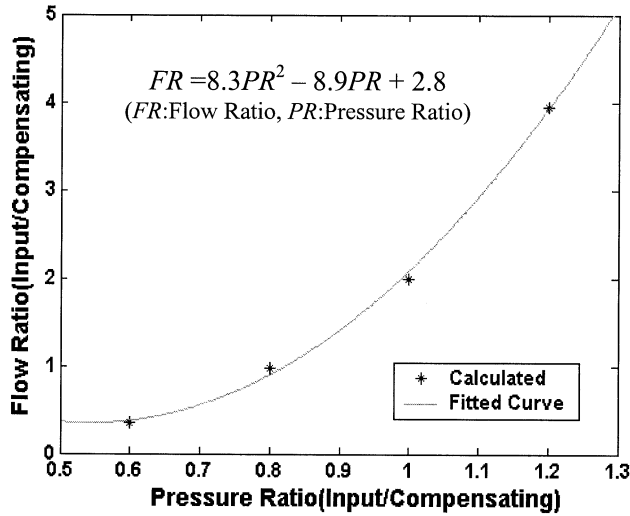


Fig. 5. Graph showing how the pressure ratio relates to the flow ratio.

$$\begin{aligned}
 y &= -0.44x + 7.3 & \left(\frac{1}{3} < x \leq 4\right) \\
 y &= -2.94x - 5.7 & (4 < x \leq 5) \text{ and} \\
 y &= 2.75 & (x > 5)
 \end{aligned}
 \tag{2}$$

where y is pH value and x is the flow ratio.

C. Modeling of Hydrogel Post and Orifice

Equilibrium swelling of the acrylic acid-hydroxyethyl methacrylate (AA/HEMA) hydrogel was investigated by monitoring the dimensional change of a hydrogel when exposed to 0.05 M phosphate buffer with pH ranging from 2 to 12 at 25 C. The total ionic strength of each buffer was adjusted to 0.3 M by the addition of a calculated amount of NaCl. The buffer solution flow rate was 100 $\mu\text{l}/\text{min}$ in a microchannel with a hydrogel post (350 μm diameter, 170 μm height). The diameter of the hydrogel post was monitored using optical microscopy. The swelling isotherm for the hydrogel is obtained as a function of pH and is similar to those previously reported [24]. The hydrogel swells in basic solutions and shrinks in acidic solutions, with the volume transition occurring between pH 4–8.

The star shaped orifice as shown in Fig. 2 has four sharp leaflets. We assumed the flow passing through the orifice is dependent on the diameter change of the hydrogel post. To make a simple model for the open orifice area, we assumed the hydrogel post moves only in the xy plane, with no shrinking or swelling in the 'z' direction due to the system constraints. From the geometry of leaflets and hydrogel post, the opening area of the orifice can be approximated from the geometric model shown in Fig. 2(b) and the following equation:

$$\text{Area} = \frac{4\alpha^3(b-r)^2}{(1+\alpha^2)^2}
 \tag{3}$$

where α is the slope of star shaped orifice, b is the diagonal length of orifice and r is the radius of the hydrogel post. Equation (3) shows that the opening area of the orifice is linearly

related to the square of the distance from the leaflet peak to the edge of hydrogel post.

IV. RESULTS

The hydrogel post was monitored through an optical microscope (BX-60, Olympus). Initially the hydrogel post swells sufficiently to seal the orifice completely and prime the system. When the input flow is initiated the hydrogel post begins to shrink, thereby allowing the compensating solution to flow again. The compensating solution travels through the orifice and enters the input channel at the T-channel junction. The time response of the hydrogel is less than two minutes and around five minutes for the system to reach equilibrium.

The lateral visualization of the hydrogel post coupled to the membrane was analyzed using a stereo-microscope as shown in Fig. 6. Fig. 6(a) shows a shrunken hydrogel post and Fig. 6(b) shows the completely swollen hydrogel post. These pictures demonstrate that the open orifice area can be correlated to the diameter of the hydrogel post taken in the plane of the top surface of the orifice as we assumed in the numerical modeling.

By using the modeled equation of each block, the total feedback control system is implemented on the Simulink platform of MatLab as illustrated in Fig. 3. The gain, k , is incorporated into the feedback loop to convert the regulated compensating flow to compensating pressure. We obtain the conversion gain from experiments and its measured value is 70. The saturator is inserted at the feedback loop to account for the limitations on compensating solution flow due to channel dimensions. The applied pressure in the compensating channel determines the maximum value of the saturator.

By using this numerical model, the pH in the output channel with the feedback loop is calculated and shows good agreement with experimentally measured data as shown in Fig. 7. This figure shows the value at the equilibrium state and the transient state is omitted. In the system with feedback, the output pH is maintained while the input pressure is varied from 30 to 50 cmH_2O and the compensating pressure is fixed at 50 cmH_2O . In the experiment, the pH is measured every two minutes. When the input pressure is more than 60 cmH_2O , the flow of acidic solution increases to the point that the compensating channel (due to channel size and driving pressure) cannot provide sufficient compensating solution to neutralize the input solution. Also when the input flow is less than 10 cmH_2O , back flow is observed in the simulation. From the simulation, the ratio between input and compensating flow at the output channel is calculated to be 4:1 when the input pressure is 60 cmH_2O .

V. DISCUSSION

The simulation uncovered phenomenon not observed experimentally such as the presence of backflow under low input flow rates. The system responded to the backflow autonomously and maintained a steady output pH value demonstrating the robustness of the design. The interactions of the orifice and hydrogel post play a key role in the successful regulation of the pH. The shape of the orifice occluded by the hydrogel greatly affects the properties of the system. However, like all control systems, the limits of the design are reached when the input flow rate is above

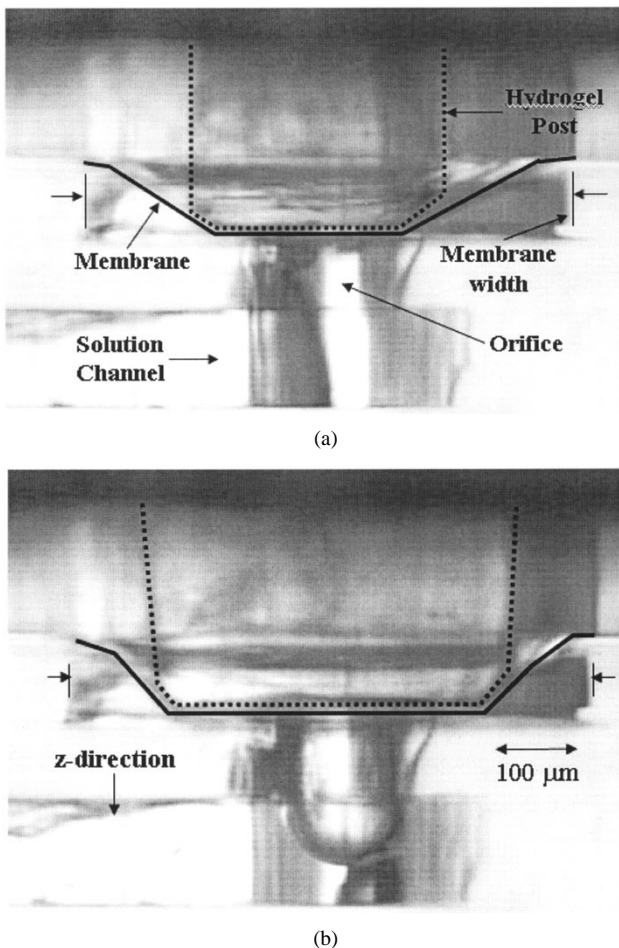


Fig. 6. Image of the lateral view of the hydrogel post (a) in the shrunken state and (b) in the swollen state coupled with a PDMS membrane. The edge of the hydrogel is shown with a dashed line and the membrane is highlighted with a solid line for clarity. Note the hydrogel only swells and shrinks in the x and y directions and not the z direction.

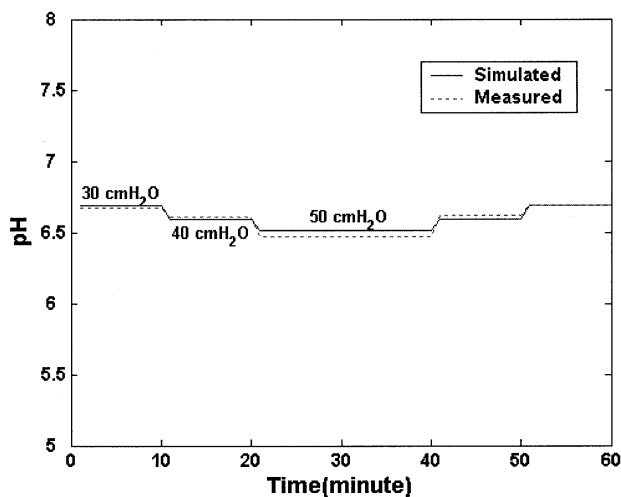


Fig. 7. Simulated and experimental output pH varying input pressures.

70 cmH₂O. The reason for this is the orifice is completely open at this elevated input flow rate and the maximum amount of compensating buffer is injected into the system.

In the simulation, the input pressure was varied between 30 to 50 in steps of 10 cmH₂O. Below 30 cmH₂O, back flow

of compensating solution occurred at the intersection of the T-channel. Fig. 8 demonstrates the velocity vector contour and experimental image at the intersection when the input pressure is 10 cmH₂O. At the intersection of the T-channel, the higher pressure region [shown in Fig. 8(b)] separates the compensating flow causing the back flow as shown in Fig. 8(a). When back flow occurs, the pH value at output channel becomes strongly basic. Even in this situation, the pH regulation system maintains constant pH after equilibrium of the hydrogel occurs demonstrating the system's ability to efficiently self-regulate under a variety of flow conditions.

The orifice and hydrogel postinteraction plays a key role in the compensating flow regulation. In earlier devices, the orifice shape was circular, but it displayed an oscillatory (unstable) response under constant input stream flow. Incorporation of the star shaped orifice produced a throttle valve functionality providing stable operation. Fig. 9 shows the opening area of the orifice according to the variation of the hydrogel post diameter. The model used a 270- μ m-radius hydrogel post because the length of the star is 270 μ m. In the case of the circular orifice, the diameter was 200 μ m. At the beginning of orifice opening, the opening area of the circular orifice is a few hundred times larger than that of the star shaped orifice. This means a rapid increase of flow in a valve with a circular shaped orifice occurs at the opening stage and, therefore, acts as an ON-OFF switch causing the oscillatory response. In contrast, the flow through a star shaped orifice continuously and smoothly changes resulting in a stable response.

The system does not effectively regulate pH once the input pressure rises above 70 cmH₂O. To neutralize the elevated input flow, an equal amount of compensating flow is required. However, the dimensions and applied pressure of compensating channel are fixed limiting the compensating flow. The saturator in the feedback loop of the model accounts for these limitations. Fig. 10 shows the output pH cannot be regulated when the input pressure is 70 cmH₂O. Without a saturator, the model predicts the output pH is regulated within a certain broader range of input conditions, but with the saturator, the pH value decreases to 3.4 at higher input pressures. A similar value is measured in experiments when the input pressure is increased to 70 cmH₂O.

VI. CONCLUSION

Organic self-regulating microsystems without electrical control components have a wide range of potential applications including low cost drug delivery devices and chronic blood or body fluid monitoring systems. The system described in this paper is made from soft materials and a single hydrogel post acts as a sensor and actuator simultaneously. The numerical model of the pH regulation system shows good correlation with the experimental data. In the pH regulation system, channel dimensions, hydrogel post and area of orifice occluded are the key factors in predicting flow regulation. In this paper, the numerical model of the T-channel, hydrogel post and orifice is presented, and the validity of the model is evaluated through experiments. The presented numerical model of the pH regulation system closely matches experimental data. The model also uncovered

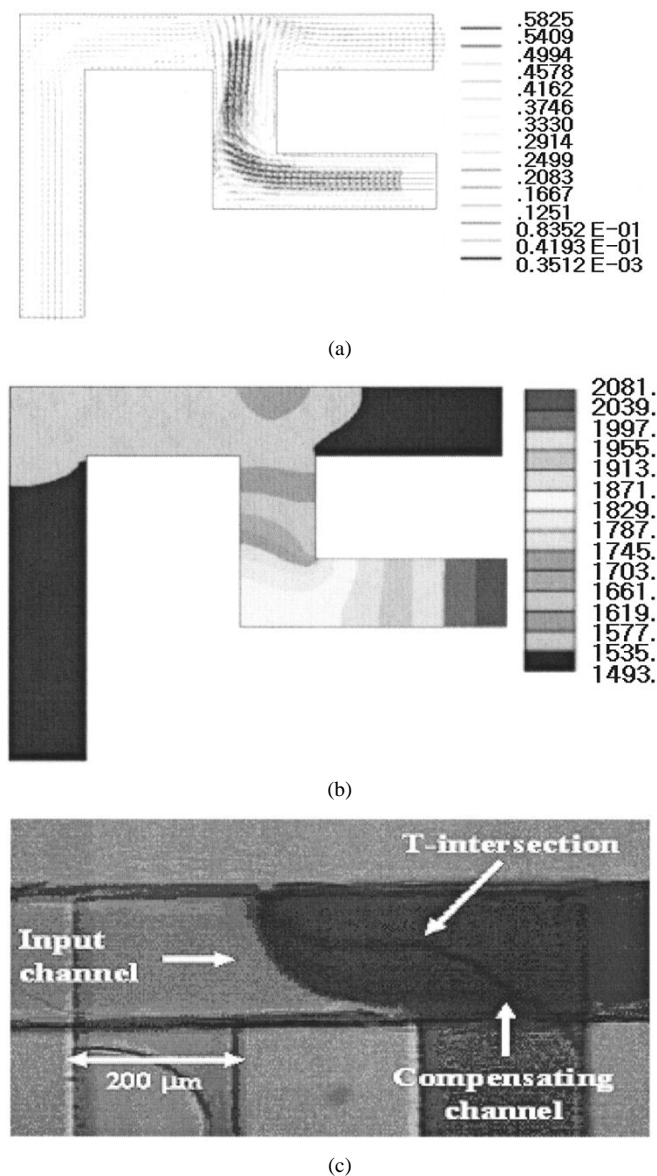


Fig. 8. Back-flow at the intersection of the T-channel. (a) Velocity vector contour—Input pressure 10 cmH₂O and (b) Pressure contour—Input pressure 10 cmH₂O. (c) The back-flow image from the optical microscope.

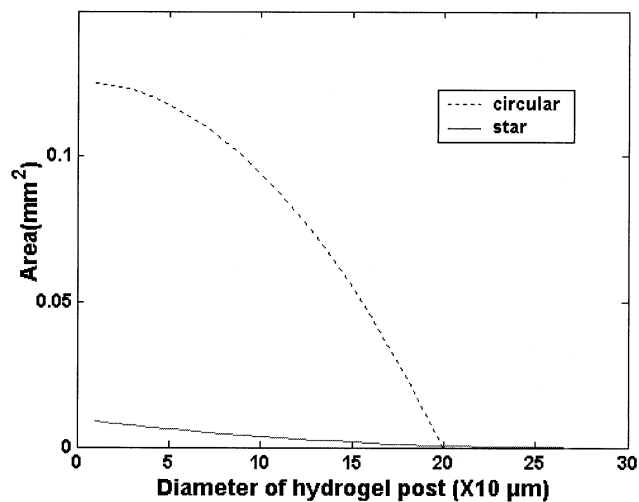


Fig. 9. Calculated opening area of circular and star-shaped orifices.



Fig. 10. Effect of saturator on the system.

previously unobserved variables and phenomenon such as back-flow, yielding a better understanding of the complete system. The model can be used for the design and analysis of alternative regulation device designs. A new regulation system could be developed using a hydrogel valve sensitive to other parameters such as temperature [16], light [19] and biologicals [20], [21]. For example, a hydrogel sensitive to biologicals, such as glucose, could be used to maintain constant blood glucose levels by regulating the amount of insulin infused into the patient.

REFERENCES

- [1] G. A. Urban and G. Jobst, "Sensor system," *Top. Current Chem.*, vol. 194, pp. 189–213, 1998.
- [2] S. Shoji, "Fluids for sensor systems," *Top. Current Chem.*, vol. 194, pp. 163–188, 1998.
- [3] A. E. Kamholz, B. H. Weigl, B. A. Finlayson, and P. Yager, "Quantitative analysis of molecular interaction in a microfluidic channel: The T-sensor," *Anal. Chem.*, vol. 71, pp. 5340–5347, 1999.
- [4] F. Sherman, S. Tung, C. J. Kim, C. M. Ho, and J. Woo, "Flow control by using high-aspect-ratio, in-plane microactuators," *Sens. Actuators*, vol. 73, pp. 169–175, 1999.
- [5] M. J. Daoura and D. R. Meldrum, "Precise automated control of fluid volumes inside glass capillaries," *J. Microelectromech. Syst.*, vol. 8, pp. 71–77, Mar. 1999.
- [6] J. Yang, Y. Huang, X. Wang, F. F. Becker, and P. R. C. Gascoyne, "Cell separation on microfabricated electrodes using dielectrophoretic/gravitational field-flow fractionation," *Anal. Chem.*, vol. 71, pp. 911–918, 1999.
- [7] D. BoIkenkamp, A. Desai, X. Yang, Y. C. Tai, E. M. Marzluff, and S. L. Mayo, "Microfabricated silicon mixers for submillisecond quench-flow analysis," *Anal. Chem.*, vol. 70, pp. 232–236, 1999.
- [8] P. J. A. Kenis, R. F. Ismagilov, and G. M. Whitesides, "Microfabrication inside capillaries using multiphase laminar flow patterning," *Science*, vol. 285, pp. 83–85, 1999.
- [9] P. C. H. Li and D. J. Harrison, "Transport, manipulation, and reaction of biological cells on-chip using electrokinetic effects," *Anal. Chem.*, vol. 69, pp. 1564–1568, 1997.
- [10] B. H. Jo, L. M. V. Lerberghe, K. M. Motsegood, and D. J. Beebe, "Three-dimensional micro-channel fabrication in polydimethylsiloxane(PDMS) elastomer," *J. Microelectromech. Syst.*, vol. 9, pp. 76–81, 2000.
- [11] D. J. Beebe, G. A. Mensing, and G. M. Walker, "Physics and applications of microfluidics in biology," *Annu. Rev. Biomed. Eng.*, vol. 4, pp. 261–286, 2002.
- [12] R. H. Liu, Q. Yu, and D. J. Beebe, "Fabrication and characterization of hydrogel-based microvalves," *J. Microelectromech. Syst.*, vol. 11, pp. 45–53, Feb. 2002.

- [13] D. Y. Jung, J. J. Magda, and I. S. Han, "Catalase effects on glucose-sensitive hydrogels," *Macromolecules*, vol. 33, pp. 3332–3336, 2000.
- [14] D. T. Eddington, R. H. Liu, J. S. Moore, and D. J. Beebe, "An organic self-regulating microfluidic system," *Lab on a Chip*, vol. 1, pp. 96–99, 2001.
- [15] W. J. Lee, "Polymer Gel Based Actuator: Dynamic Model of Gel for Real Time Control," Ph.D. dissertation, MIT.
- [16] J. Hoffmann, M. Plotner, D. Kuckling, and W. J. Fischer, "Photopatterning of thermally sensitive hydrogels useful for microactuators," *Sens. Actuators*, vol. 77, pp. 139–144, 1999.
- [17] G. Chen, Y. Imanishi, and Y. Ito, "PH-Sensitive thin hydrogel microfabricated by photolithography," *Langmuir*, vol. 14, pp. 6610–6612, 1998.
- [18] T. Tanaka, I. Nishio, S.-T. Sun, and S. Ueno-Nishio, "Collapse of gels in an electric field," *Science*, vol. 218, pp. 467–469, 1982.
- [19] A. Suzuki and T. Tanaka, "Phase transition in polymer gels induced by visible light," *Nature*, vol. 346, pp. 345–347, 1990.
- [20] K. Kataoka, H. Miyazaki, M. Bunya, T. Okano, and Y. Sakurai, "Totally synthetic polymer gels responding to external glucose concentration: Their preparation and application to on-off regulation of insulin release," *J. Amer. Chem. Soc.*, vol. 120, pp. 12 694–12 695, 1998.
- [21] T. Miyata, N. Asami, and T. Uragami, "A reversibly antigen-responsive hydrogel," *Nature*, vol. 399, pp. 766–769, 1999.
- [22] N. Kato, F. Takahashi, and S. Yamanobe, "Property of magneto-driven poly (*N*-isopropylacrylamide) gel containing γ -Fe₂O₃ in NaCl solution as a chemomechanical device," *Mater. Sci. Eng., C: Biomater. Mater. Sens. Syst.*, vol. C5, pp. 141–147, 1997.
- [23] N. A. Peppas, *Hydrogels in Medicine and Pharmacy*. Boca Raton, FL: CRC, 1986, vol. 1.
- [24] S. K. De, N. R. Aluru, B. Johnson, W. C. Crone, D. J. Beebe, and J. Moore, "Equilibrium swelling and kinetics of pH-Responsive hydrogels: Models, experiments, and simulations," *J. Microelectromech. Syst.*, vol. 11, pp. 544–555, Oct. 2002.
- [25] D. J. Beebe, J. S. Moore, J. M. Bauer, Q. Yu, R. H. Liu, C. Devadoss, and B. H. Jo, "Functional structures for autonomous flow control inside microfluidic channels," *Nature*, vol. 404, pp. 588–590, 2000.



Sanghoon Lee received the B.S. degree in electrical engineering and the M.S. and Ph.D. degrees in biomedical engineering from the Seoul National University, Seoul, Korea, in 1983, 1987, and 1992, respectively.

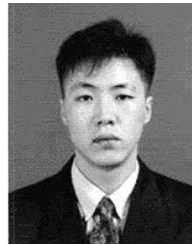
From 1992 to 1998, he was an Instructor and Assistant Professor, and is currently an Associate Professor in the Department of Biomedical Engineering at the Dankook University, Korea. From 1985 to 1992, he was a Researcher in the Department of Biomedical Engineering at the Seoul National University Hospital.

He was Visiting Scientist in the Department of Biomedical Engineering at the University of Wisconsin-Madison, in 2002. He had broad interests in biomedical instrumentation and the development and use of microdevices for applications in medicine and biotechnology. His current interests are the development of single cell handling and analysis of microfluidic devices and flexible implantable sensor for medical applications.



David T. Eddington received the B.S. degree in materials science and engineering from the University of Illinois at Urbana-Champaign in 2000 and the M.S. degree in biomedical engineering from the University of Wisconsin-Madison in 2002. He is currently pursuing the Ph.D. degree in biomedical engineering from the University of Wisconsin-Madison.

His research interests include the development of systems to facilitate drug delivery such as regulation systems, micropumps, and closed-loop infusion systems.



Young-Min Kim received the B.S. and M.S. degrees in mechanical engineering from Hanyang University in 1997 and 1999, respectively, and has been working toward the Ph.D. degree in mechanical engineering at the Hanyang University, Seoul, Korea, since 1999. He worked on planer flow casting as his Master's thesis.

His current research interests include microscale heat transfer and fluid mechanics, microfluidics, bio-MEMS and MEMS device such as micromixer and microchannel.



Woo-Seung Kim received the B.S. degree in mechanical engineering from Hanyang University, Seoul, Korea, in 1981 and the M.S. and Ph.D. degrees in mechanical engineering from North Carolina State University, Raleigh, in 1986 and 1989, respectively.

From 1989 to 1991, he was a Research Associate in North Carolina State University. Currently, he is a Professor of Mechanical Engineering at the Hanyang University, Ansan, Korea.



David J. Beebe (S'89–M'95) received the B.S., M.S., and Ph.D. degrees in electrical engineering from the University of Wisconsin-Madison, in 1987, 1990, and 1994, respectively.

He is an Associate Professor in the Department of Biomedical Engineering at the University of Wisconsin-Madison with joint appointments in Electrical and Computer Engineering and Mechanical Engineering. He is also a member of the University of Wisconsin Comprehensive Cancer Center, Vascular Biology Program and Biotechnology Training Program.

From 1996 to 1999, he was an Assistant Professor in the Department of Electrical and Computer Engineering and an Assistant Research Professor in the Beckman Institute for Advanced Science and Technology at the University of Illinois at Urbana-Champaign. From 1994 to 1996, he was an Assistant Professor at Louisiana Tech University. From 1991 to 1994, he was an NIH Biotechnology Predoctoral Trainee. He has broad interests in biomedical instrumentation and the development and use of microfabricated devices for applications in medicine and for the study of biology. His current interests include technology development for the handling and analysis of biological objects, development of nontraditional autonomous micro fluidic devices and systems, and the study of cell and embryo development in microenvironments.